LncRNA Profiling of Exosomes Derived From Staphylococcus Aureus-induced Bovine Mammary Epithelial Cell Lines MAC-T

Yu Chen
Huazhong Agricultural University: Huazhong Agriculture University
Hongyuan Jing
Northeast Agricultural University
Miaoyu Chen
Huazhong Agricultural University: Huazhong Agriculture University
Wan Liang
Huazhong Agricultural University: Huazhong Agriculture University
Mengyao Guo (guomy1985@163.com)
Northeast Agricultural University https://orcid.org/0000-0003-0426-2203

Research

Keywords: mastitis, Staphylococcus aureus, exosome, lncRNA

Posted Date: September 16th, 2020

DOI: https://doi.org/10.21203/rs.3.rs-72267/v1

Abstract

Background: Exosomes (carrying proteins, miRNA, lncRNA, etc.) play a vital role in participating in the occurrence and development of mastitis. LncRNA can play a variety of regulatory roles by combining with protein, RNA, and DNA. The expression of mRNA and lncRNA in exosomes derived from bovine mammary epithelial cells infected by *S. aureus* is rarely understood.

Methods: We used ultracentrifugation to separate exosomes derived from *S. aureus*- stimulated MAC-T cells. After extracting exosomal RNA, RNA sequencing was performed. We screened differentially expressed genes, mRNA and lncRNA, and predicted their functions through KEGG and GO analysis. 6 mRNA and lncRNA were randomly selected for RT-qPCR verification.

Results: Analysis of the sequencing results showed that there were 186 differentially expressed genes, 431 differentially expressed mRNAs and 19 differentially expressed lncRNAs in the exosomes derived from *S. aureus*-infected and non-infected MAC-T acells. By predicting lncRNA target genes, it was found that 19 differentially expressed lncRNAs all acted on multiple mRNAs in cis and trans. GO analysis revealed that differentially expressed genes and lncRNA target genes played significant roles in such metabolism, transmembrane transport, cellular response to DNA damage stimulus, response to cytokines. KEGG enrichment indicated that lncRNA target genes gathered in the TNF pathway, Notch pathway, phosphatidylinositol signaling system and p53 pathway.

Conclusion: The data suggested that *S. aureus* induced changes in genes, mRNA, and lncRNA in exosomes secreted by MAC-T cells, which furtherly triggered other cells damage through exosomal delivery. This study would provide valuable resource for understanding the lncRNA information in exosomes derived from dairy cow mammary epithelial cells, and conduced to the study of *S. aureus* infection in dairy cow mammary glands.

Introduction

Mastitis is a common and widespread infectious disease in dairy farms all over the world, which characterized by inflammation of the mammary glands, resulting in a decrease in milk production and quality [1–3]. There are many kinds of pathogens of mastitis, and *Staphylococcus aureus* (*S. aureus*) is one of the important pathogens in subclinical mastitis[4]. *S. aureus* often causes clinical or subclinical mastitis, and the intramammary infections are usually characterized as mild, chronic or persistent [5].

Bovine mammary epithelial cells (BMEC) are not only essential for the synthesis of milk components, but also the main line of defense against pathogen invasion [3, 6]. Milk contains a large number of exosomes, which are mainly derived from BMEC. The cargo carried by milk exosomes has been suggested to play a role in cell growth, development, immune regulation and regulation [7]. Exosomes are tiny extracellular vesicles with a diameter ranging from 40–150 nm, which originate from the internal vesicles of multivesicles in almost all cell types [8]. Typical exosomes are surrounded by phospholipid membranes, which contain proteins, lipids and nucleic acid molecules (including miRNA, cicrRNA, lncRNA, etc) [9]. With the deepening of the understanding of exosomes, exosomes are used as carriers to deliver drugs for targeted therapy. Because exosomes have been proven to tolerate the harsh environment in the intestine, are absorbed by various cell types, cross biological barriers and reach surrounding tissues [7]. Exosomes can also initiate a signal cascade of neighboring cells through the paracrine pathway. Therefore, it is very valuable to explore the RNA sequence in exosomes derived from MAC-T cells infected by *S. aureus*.

Long non-coding RNA (lncRNA) is a type of RNA that does not have the ability to encode proteins with more than 200 nucleotides in length [10]. LncRNA can bind to DNA, RNA, and proteins to play a role by mediating DNA methylation, mRNA degradation, chromatin remodeling, histone modification and protein modification [10, 11]. There have been research evidences that lncRNA plays a key role in mastitis caused by *S. aureus*, *Escherichia coli*, *Mycoplasma bovis* and other pathogens though regulating the expression of specific genes. LRRC75A-AS1 in bovine mammary epithelial cells and breast tissue was down-regulated under inflammatory conditions, and knocking out LRRC75A-AS1 in MAC-T cell line inhibited the adhesion and invasion of *S. aureus* and attenuated the activation of the NF-κB pathway [12]. LncRNA-TUB was higher expression in the mammary epithelial cells of dairy cows that received pro-inflammatory stimulation, and knockout of lncRNA-TUB indicated that it played a key role in the morphology, proliferation, migration and β-casein secretion of mammary epithelial cells [13].

Due to the spongy effect of exosomes, we speculated that the expression profile of lncRNA had changed in the exosomes derived from MAC-T cells infected with *S. aureus*. The purpose of this study was to determine the expression profile of lncRNA in exosomes derived from *S. aureus*-infected and non-infected MAC-T cells to provide new targets for the link between bovine mastitis caused by *S. aureus* and lncRNA for future research.

Methods

Cell culture and supernatant collection

The bovine mammary epithelial cell line MAC-T was cultured in DME/F-12 (1:1) medium (Hyclone, USA) supplemented with 5 mmol/L L-glutamine (BioSharp, China), 5 μg/mL insulin (BioSharp, China), 1 μg/mL hydrocortisone (Sigma-Aldrich, USA), 100 U/mL penicillin/100 μg/mL streptomycin (Invitrogen, USA) and 10% exosome-depleted fetal bovine serum (ExoDP-FBS; Gibco, USA) at 37 °C with 5% CO2 incubator. *S. aureus* CVCC3051 strain, obtained from China Veterinary Culture Collection (CVCC), was grown in tryptone soy broth medium until mid-log phase. After colony forming units (CFU) calculated, *S. aureus* was inactivated in hot water bath at 80 °C for 30 minutes. When MAC-T cells were approximately 60–70% confluent in the T-75 cell flask, *S. aureus* was inoculated into the cell flask at a multiplicity of infection (MOI) of 100. After 24 hours of culture, the cell supernatant was collected for separation of exosomes.

Exosomes isolation

Cell line exosomes were separation by ultracentrifugation as previously described [14]. The cell supernatant was sequentially subjected to 300 × g, 10 min; 2000 × g, 10 min; 10,000 × g, 30 min in a large-capacity high-speed centrifuge (AVANTI J-26XPN, Beckman, USA). After collecting the supernatant, ultra-high-speed centrifuge with SW32Ti rotor (optima XE-90, Beckman, USA) was hired to ultracentrifuge at 100,000 × g for 70 min. Pellet was collected and resuspended in PBS, and then perform ultracentrifugation again at 100,000 × g for 70 min. Finally, the exosomal pellet was resuspended in PBS and collected for subsequent analysis.

Transmission electron microscopy

Exosomes were mixed with an equal volume of 4% paraformaldehyde. 100 μl mixed liquid was sucked off and added dropwise to the copper net, then phosphotungstic acid was added for negative staining. After drying, transmission electron microscope was used to observe exosomal morphology at 80 kV.

Particle size distribution assay

Exosomes obtained by ultracentrifugation was diluted by PBS to the optimal concentration for analysis. ZETASIZER Nanoparticle Tracking Analysis (NTA) instrument (Malvern, Worcestershire, England) was performed to analyze particle size of exosome. According to the Stokes-Einstein principle, dynamic light scattering detected Brownian motion of particles to generate trajectories and displacements to determine particle size distribution.

Flow cytometry analysis

Exosomes acquired by ultracentrifugation separation were incubated with CD63 (#557288, BD Bioscience) or CD81 (#555676, BD Bioscience), and exosomes without antibody incubation was used as a negative control. BD accuri C6 flow cytomenter was used for sample detection according to the operating instructions, and then analyzed with FlowJo software.

RNA extraction and lncRNA sequencing

Total RNA was extracted from exosomal samples using Trizol reagent (Invitrogen, Carlsbad, CA). Total RNA is used as input material for constructing cDNA library. Mainly, exosomal trace RNA purification, cDNA synthesis through reverse transcription, end repair and adaptor, PCR amplification and other steps to build a library, and then go through the library quality inspection and sequence on an Illumina HiSeq 4000 platform (Illumina Inc., San Diego, CA).

Sequence data quality control

The original image file (BCL) obtained by sequencing was converted into raw data in FASTQ format after base recognition. Quality analysis on the original data was performed to assess whether it was suitable for bioinformatics analysis. Quality analysis mainly included sequencing quality and base composition analysis. Clean data was obtained by removing linker sequence and low quality sequence from raw data. The quality of clean data was then evaluated using FASTQC v0.10.1.

Reference genome alignment and genome-wide reads distribution map

Clean reads were obtained through filtering sequencing data by Trimmomatic (Version 3) and removing ribosomal RNA by Bowtie2 (v2.2.5). Bowtie2 (v2.2.5) was used to generate the index of the reference genome, and alignment of paired-end clean reads to the reference genome was performed with HISAT2 (v2.1.0). The assembly of mapped transcripts for each sample was performed with Scripture (beta2) and Cufflinks (v2.1.1) in a reference-based approach[15].

Differential expression analysis

Quantitative analysis of genes and transcripts was performed via htseq v0.11.2. DESeq2 (1.18.1) is used to determine differential expression in transcripts or gene expression data. It is determined that the transcripts or genes with P value < 0.05 are differentially expressed in biological replication. Q value < 0.05 and |log2 (fold change)|<1 are considered as thresholds for significant differential expression in abiotic replication.

Prediction of lncRNA-gene interactions

In order to predict the targets of lncRNAs in MAC-T cells and thus understand potential functions of lncRNAs. Method as in previous research[15]. Firstly, we searched the 10 k/100 k coding genes upstream and downstream of lncRNA to find cis role lncRNA. Then construction logarithm was modeled as log (P / (1- P)) = a + bx + cy, where a, b and c were model parameters, y represented the percentage of GC content in the sequence, and P represents

lncRNA binding to a 10 kb long sequence the odds ratio. Predict statistical significance by using Wald test on Z statistics (p value < 0.05). Only lncRNAs with p value < 0.05 and z score > 0 were annotated as trans lncRNA.

Kyoto encyclopedia of genes and genomes (KEGG) biological pathway enrichment and Gene ontology (GO) functional enrichment analysis

The GOseq R package was used to analyze GO enrichment for differentially expressed genes or lncRNA target genes [15]. GO terms with Q values < 0.05 were considered significantly enriched by differentially expressed genes. The summary differential expression genes and lncRNA target genes in KEGG pathways enrichment was analyzed by KOBAS (v3.0) software.

RT-qPCR validation

Total exosomal RNA samples from *S. aureus*-infected and non-infected MAC-T cells for the lncRNA-seq were analyzed by RT-qPCR. Then cDNA was obtained by reverse transcriptase reagent according to the instruction manual. The qPCR was performed using the SYBR Green Plus Reagent Kit with the Light Cycler 96 instrument (Roche, Basel, Switzerland) following the instructions of the manufacturer. GAPDH was used as an internal reference gene. The fold change of mRNA transcripts and lncRNAs was calculated using $2^{-\Delta\Delta Cq}$ methods.

Statistical analysis

IBM SPSS 20 was used to perform statistical analyses. One-Way Analysis of Variance (ANOVA) was performed to detect statistically differences in lncRNAs and mRNAs between *S. aureus* infected and non-infected groups. $p < 0.05$ and $p < 0.01$ were considered as significant differences.

Results

Identification of exosomes

In order to directly observe the morphology of exosomes, we employed transmission electron microscopy to observe negatively stained exosomes samples. As shown in Fig. 1A, it had a very obvious single-layer membrane structure under the electron microscope, which appeared as a saucer-shaped or disc-shaped vesicle with one side recessed. NTA analysis was performed to further determine the size of exosomes. The main peak of the particle size of the exosomes we separated was 70.55 nm, and the 80.3% particle size was between 40–150 nm (Fig. 1B). Flow cytometry was used to detect the surface characteristic markers of exosomes. The results revealed that the positive rates of CD81 and CD63 were 92.7% and 85.9%, respectively (Fig. 1C).

Sequencing data statistics of exosomes derived from MAC-T cells

In the current study, a total of 4 cDNA libraries were constructed by isolating total RNA from exosomes derived from *S. aureus*-infected and non-infected MAC-T cells. The raw reads in the cDNA library of different samples were cont1, 67572136; cont2, 66474707; infect1, 69033293; infect2, 70292999. GC content (%) percentages were found to be cont1, 48.61; cont2, 47.63; infect1, 49.75; infect2, 49.98 (Table 1). We conducted quality control analysis on raw data, and the results are as follows. The quality of the bases in raw reads was counted in each sequencing cycle. The base composition of each cycle is shown in Fig. 2A. As shown in Fig. 2B, the blue line represented the average base quality of the cycle in the base quality distribution box plot. Base error rate is limited to 0.11–0.13 in raw reads

(Fig. 2C). We filtered raw data to get clean data, and clean reads, GC%, Q20, Q30, clean bases were counted in Table 2, and the quality control results of clean reads were shown in Fig. 2D, E and F. In addition, when the clean reads were aligned with the bovine reference genome using HISAT2 software by an improved BWT algorithm (FM index), it was determined that the Total Mapped Reads or Fragments belonging to all the samples was above 80% and was mapped in the reference genome (Table 3).

Table 1 Statistics of raw data quality

Sample name	Total reads	Total reads (bp)	GC%	Error rate(%)	Q20(%)	Q30(%)
cont1	67572136	10135820400	48.61	0.11	98.64	96.29
cont2	66474707	9971206050	47.63	0.11	98.75	96.62
infect1	69033293	9854993950	49.75	0.13	98.26	95.53
infect2	70292999	10543949850	49.98	0.13	98.33	95.57

Note: Total reads: Statistics of total reads, each adjacent four lines contains the information of one read, and the total read number of each file is calculated; **Total base:** The number of all bases in total data; **Clean reads:** Filter the original data, remove the linker sequence, remove the contaminated part, and remove the sequence containing more low-quality bases to obtain clean reads; **GC%:** The percentage of G and C in all bases; **Error rate:** The error rate of sequencing; **Q20, Q30:** The percentage of total number of bases where the Phred score is greater than 20 and 30 which indicates base call accuracy.

Table 2 Summary of filter data

Sample name	Raw reads	Raw bases	clean reads	GC%	Q20(%)	Q30(%)	Clean bases	Clean bases%
cont1	67572136	10135820400	65650056	48.57	99.16	97.32	9689017234	95.59
cont2	66474707	9971206050	65006370	47.54	99.22	97.52	9514596643	95.42
infect1	69033293	9854993950	65789887	49.67	98.95	96.74	9383925239	95.22
infect2	70292999	10543949850	68826092	49.91	98.94	96.69	10102208096	95.81

Note: Raw reads: Statistics of raw reads, each adjacent four lines contains the information of one read, and the total read number of each file is calculated; **Raw base:** The number of all bases in raw data; **Clean reads:** Filter the original data, remove the linker sequence, remove the contaminated part, and remove the sequence containing more low-quality bases to obtain clean reads; **GC%:** The percentage of G and C in all bases; **Q20, Q30:** The percentage of total number of bases where the Phred score is greater than 20 and 30 which indicates base call accuracy; **Clean bases:** The number and length of sequences in clean reads calculate the number of bases; **Clean bases%:** Percentage of Clean bases/Raw base.

Table 3 Summary of reads mapped to reference genome

Sample name	cont1	cont2	infect1	infect2
The effective reads	112941906 (100%)	123138246 (100%)	86025798 (100%)	107088594 (100%)
Total mapped	5194592 (4.60%)	3683147 (2.99%)	4047510 (4.70%)	3269932 (3.05%)
Multiple mapped	550374 (0.49%)	253166 (0.21%)	492395 (0.57%)	411581 (0.38%)
Uniquely mapped	4644218 (4.11%)	3429981 (2.79%)	3555115 (4.13%)	2858351 (2.67%)
Read1 mapped	2600145 (2.30%)	1843109 (1.50%)	2022180 (2.35%)	1633528 (1.53%)
Read2 mapped	2594447 (2.30%)	1840038 (1.49%)	2,025,330 (2.35%)	1636404 (1.53%)
Reads map to '+'	2,599,952 (2.30%)	1842749 (1.50%)	2025784 (2.35%)	1636402 (1.53%)
Reads map to '-'	2594640 (2.30%)	1840398 (1.49%)	2,021,726 (2.35%)	1633530 (1.53%)
Reads mapped in proper pairs	4815452 (4.26%)	3470648 (2.82%)	3800530 (4.42%)	3059418 (2.86%)

Note: The effective reads: The remaining number of clean reads after removing rRNA reads will be used for subsequent genome alignment; **Total mapped:** The number of sequencing sequences that can be aligned on the genome; **Multiple mapped:** The number of sequencing sequences with multiple alignment positions on the sequence of reference; **Uniquely mapped:** the number of sequencing sequences with unique alignment positions on the reference sequence; **Read-1, Read-2 mapped:** Pair end sequence, whose two parts that can be located on the number of genome respectively, the statistical ratio of the two parts should be roughly the same; **Reads map to'+':** The number of reads aligned to the positive strand of the genome; **Reads map to'-':** The number of reads aligned to the genome on the negative strand; **Reads mapped in proper pairs:** The relative distance of the pair end sequence mapping to the genome conforms to the length distribution of the sequenced fragments.

Distribution of reads in the chromosomes and known types of RNAs

After mapped in the reference genome, we counted the position information of the genomes corresponding to all reads to evaluate the depth of sequencing data coverage. The distribution of reads on each chromosome was displayed in Fig. 3A. Subsequently, the reads aligned on the chromosome were annotated to exonic, intronic, and

intergenic. Reads compared to the genome was counted the distribution (Fig. 3B). And the reads distributions in the known RNA types were shown in Fig. 3C.

Differentially expressed genes analysis in exosomes derived from S. aureus**-infected and non-infected MAC-T cells**

DESeq2 was used to screen differentially expressed genes. We selected the differentially expressed genes between samples through the two levels of multiple of difference (|log2(Fold Change)|>1) and significance level (Q value < 0.05) [16–18]. The statistics of the number of differentially expressed genes in exosomes derived from *S. aureus*-infected and non-infected MAC-T cells were shown in Fig. 4A. There were a total of 186 genes expression disorders, of which 31 genes were significantly up-regulated and 155 genes were significantly down-regulated. We used the RPKM/COUNT of the differential gene as the expression level. Hierarchical Clustering analysis was performed to cluster genes with the same or similar expression patterns into clusters, and used different colored regions to represent different clustering grouping information to determine clustering mode of different sample control modes [15, 19]. In this study, the hierarchical clustering analysis of differentially expressed genes is shown in Fig. 4B.

GO enrichment analyses were conducted to search for the biological processes, cellular components, and molecular functions of differentially expressed genes in more detail [15, 20]. GO analysis was performed on the up-regulated and down-regulated genes. According to the enrichment point, all disordered genes are classified according to GO terms (Fig. 4C and D). Moreover, KEGG pathway analysis results were calculated according to the enrichment points, and the best gene pathways related to the up-regulated and down-regulated genes were listed in Fig. 4E and F.

Differentially expressed mRNAs and lncRNAs analysis in exosomes derived from S. aureus**-infected and non-infected MAC-T cells**

The expression level of the transcript was calculated using the RPKM value. We found that there were 78 up-regulated and 353 down-regulated known mRNAs, and 8 up-regulated and 11 down-regulated lncRNAs (Fig. 5A and B). Up-regulated lncRNAs were XR_003034773.1, XR_810477.3, XR_003031139.1, XR_003038102.1, XR_003034201.1, XR_236621.4, XR_003031133.1 and XR_003031134.1; down-regulated lncRNAs were XR_003034734.1, XR_003033312.1, XR_003033314.1, XR_003034774.1, XR_003035599.1, XR_003033311.1, XR_001500758.2, XR_003029422.1, XR_003034775.1, XR_003031994.1 and XR_003036684.1. In addition, the differentially expressed mRNAs and lncRNAs were also clustered in the hierarchical cluster analysis map (Fig. 5C, D).

Prediction of lncRNA target genes and mRNAs

The mode of action of lncRNA regulating target genes could be divided into two categories: cis regulation (In Cis) and trans regulation (In Trans). We made predictions about how the differentially expressed lncRNAs regulated the target genes (Additional file 1 & 2). Differentially expressed lncRNAs were selected to draw a network diagram of the interaction between these lncRNAs and their target genes (Fig. 6), so as to provide reference and help for the overall analysis of the functions of lncRNAs in samples.

GO enrichment and KEGG enrichment analysis of lncRNA target genes and mRNAs

GO analysis was performed on the target gene, and take the $P < 0.05$ of GO annotation enrichment as the significance threshold. GO terms of biological processes, cellular components and molecular functions were shown 10 GO terms, respectively (Fig. 7A). The Additional file for detailed biological processes, cell components and molecular functions were seen in Additional file 3, 4 and 5. KEGG analysis was performed on the target gene, and use the $P < 0.05$ of the enrichment degree of KEGG pathway as the significance threshold to obtain the analysis result. KEGG enriched target gene pathways were classified according to environmental information processing, human diseases, metabolism, and biological systems. It was found that lncRNA target genes were most closely related to human diseases (Fig. 7B). KEGG pathway analysis results are shown in the bubble diagram of the KEGG pathway (Fig. 7C). Multiple target genes are involved in the TNF signaling pathway, Notch signaling pathway, Phosphatidylinositol signaling system and p53 signaling pathway in the KEGG target gene enrichment pathway.

Results of RT-qPCR validation was in accordance with RNA-Seq

6 differentially expressed mRNAs (BRSK2, PRKDC, FAT3, SFMBT1, SLF2 and LCOR) and 6 differentially expressed lncRNAs (XR_001500758.2, XR_003029422.1, XR_003036684.1, XR_003034201.1, XR_003034734.1 and XR_003038102.1) were chosen to verify the lncRNA-seq results. The results of qPCR were found to be in accordance with RNA-seq (Fig. 8A, B), suggesting that RNA-seq results were reliable.

Discussion

Mastitis is an inflammation of the udders of dairy cows that is almost always caused by pathogenic microorganisms[21]. It seriously harms dairy farming and the dairy industry. Cow mammary epithelial cells can produce exosomes and excrete with milk during lactation, and exosomes can also communicate between cells through paracrine pathways. The cargo carried in the exosomes is the switch that initiates communication. The aim of this study was to investigate the expression of mRNA and lncRNA in exosomes derived from bovine mammary epithelial cells infected by *S. aureus* (Fig. 9).

In this study, we used ultracentrifugation to separate the exosomes in the MAC-T cell culture medium. We directly observed saucer-shaped vesicles through transmission electron microscopy. The NTA instrument detected 80% of the extracellular vesicles with a size of 40–150 nm. In addition, the positive rates of CD81 and CD63, which are characteristic markers on the surface of exosomes, were more than 80% by flow cytometry. All the above data implied that exosomes were successfully isolated.

After the total exosomal RNA extracted, high-throughput sequencing was performed on the Illumina platform to reveal the lncRNA and gene expression profiles in the exosomes derived from *S. aureus* infected and non-infected MAC-T cells. It was found that186 differentially expressed genes, 431 differentially expressed mRNAs and 19 differentially expressed lncRNAs were screened out. The function of most of these lncRNAs was unclear. Usually, we predicted the function of lncRNA based on its closely related coding genes [22]. In this study, we first estimated the target genes of differentially expressed lncRNA using cis and trans, then GO and KEGG analysis were performed on the target gene to find the potential role of lncRNA [15]. We found that these differentially expressed target genes were mainly related to inflammation or apoptosis signaling pathways through enrichment analysis of GO and KEGG pathways and coding-non-coding co-expression network analysis.

Differentially expressed lncRNA XR_001500758.2 and XR_003029422.1 were enriched in TNF signaling pathway, Notch signaling pathway, Phosphatidylinositol signaling system p53 signaling pathway, RIG-I-like receptor

signaling pathway, MAPK signaling pathway and PI3K-Akt signaling pathway. These signaling pathway are closely related to inflammation or apoptosis. The target genes predicted for XR_001500758.2 included ATM, FAS, SERPINB5, PPIP5K2, SNW1, MLKL, IL1A, PLA1A. The target genes predicted for XR_003029422.1 included MAML2, GORAB, DGKH, DGKI, SELE, ITGA1. ATM protein kinase is a product encoded by the telangiectasia ataxia mutated gene ATM, which senses DNA damage, transmits DNA damage signals to downstream target genes, initiates stress systems and produces cycle arrest, cell repair and apoptosis[23, 24]. FAS, adapter proteins associated with the death domain (FADD and TRADD) belongs to TNFR family. FAS could activate NF-kappa B, MAPK and PI3K-Akt signaling pathway. Based on predictions, we found that lncRNA had multiple targets and was involved in the complex process of regulating the immune response.

Conclusion

In conclusion, the molecular mechanism of *S. aureus* infecting dairy cow mammary epithelial cells involves the paracrine mode of exosomal cargo lncRNA playing a regulatory role in the TNF pathway, Notch pathway, Phosphatidylinositol signaling system and p53 pathway. The data obtained in this study would also provide valuable resource for understanding the lncRNA information in exosomes derived from dairy cow mammary epithelial cells, and conduced to the study of *S. aureus* infection in dairy cow mammary glands.

Abbreviations

BMEC
Bovine mammary epithelial cells; CFU:Colony forming units; GAPDH:glyceraldehyde-3-phosphate dehydrogenase; GO:Gene ontology; KEGG:Kyoto encyclopedia of genes and genomes; LncRNA:Long non-coding RNA; MOI:Multiplicity of infection; NTA:Nanoparticle tracking analysis; RPKM:Reads Per Kilobase per Million mapped reads; RT-qPCR:Real-time quantitative polymerase chain reaction; S. aureus:Staphylococcus aureus.

Declarations

Acknowledgments

Not applicable.

Authors' contributions

Y.C. and M.G. conceived the study; Y.C., H.J., M.C., W.L., and M.G. carried out experiments and data analysis; Y.C., H.J., and M.G. interpreted the data. Y.C. and M.G. wrote the manuscript. All authors approved the final version. The authors declare that no conflicts of interest exist.

Funding

Not applicable.

Availability of data and materials

Research data are listed in the supplementary data set.

Ethics approval and consent to participate

Not applicable.

Consent for publication

Not applicable.

Competing interests

The authors declare that they have no competing interests.

Author details

[1] College of Veterinary Medicine, Northeast Agricultural University, Harbin 150030, People's Republic of China. [2] College of Veterinary Medicine, Huazhong Agricultural University, Wuhan 430070, People's Republic of China.

References

1. Wilson DJ, Gonzalez RN, Das HH. Bovine mastitis pathogens in New York and Pennsylvania: prevalence and effects on somatic cell count and milk production. J Dairy Sci. 1997;80(10):2592–8.
2. Yang F, Zhang S, Shang X, Wang L, Li H, Wang X. Characteristics of quinolone-resistant Escherichia coli isolated from bovine mastitis in China. J Dairy Sci. 2018;101(7):6244–52.
3. Sun X, Luo S, Jiang C, Tang Y, Cao Z, Jia H, et al. Sodium butyrate reduces bovine mammary epithelial cell inflammatory responses induced by exogenous lipopolysaccharide, by inactivating NF-κB signaling. Journal of dairy science. 2020; S0022-0302(20)30504-X.
4. Rossi BF, Bonsaglia ÉCR. First investigation of Staphylococcus argenteus in a Brazilian collections of S. aureus isolated from bovine mastitis. BMC Vet Res. 2020;16(1):252.
5. Niedziela DA, Murphy MP, Grant J, Keane OM, Leonard FC. Clinical presentation and immune characteristics in first-lactation Holstein-Friesian cows following intramammary infection with genotypically distinct Staphylococcus aureus strains. Journal of dairy science. 2020; S0022-0302(20)30491-4.
6. Swanson KM, Stelwagen K, Dobson J, Henderson HV, Davis SR, Farr VC, et al. Transcriptome profiling of Streptococcus uberis-induced mastitis reveals fundamental differences between immune gene expression in the mammary gland and in a primary cell culture model. J Dairy Sci. 2009;92(1):117–29.
7. Sanwlani R, Fonseka P, Chitti SV, Mathivanan S. Milk-Derived Extracellular Vesicles in Inter-Organism, Cross-Species Communication and Drug Delivery. Proteomes. 2020;8(2):11.
8. Mohan A, Agarwal S, Clauss M, Britt NS, Dhillon NK. Extracellular vesicles: novel communicators in lung diseases. Respiratory research. 2020;21(1):175.
9. Frydrychowicz M, Kolecka-Bednarczyk A, Madejczyk M, Yasar S, Dworacki G. Exosomes - structure, biogenesis and biological role in non-small-cell lung cancer. Scandinavian journal of immunology Scandinavian journal of immunology. 2015;81(1):2–10.
10. Li X, Wang H, Zhang Y, Zhang J, Qi S, Zhang Y, et al. Overexpression of lncRNA H19 changes basic characteristics and affects immune response of bovine mammary epithelial cells. PeerJ. 2019;7:e6715.

11. Lodde V, Murgia G, Simula ER, Steri M, Floris M. Long Noncoding RNAs and Circular RNAs in Autoimmune Diseases. Biomolecules. 2020;10(7):E1044.
12. Wang X, Wang H, Zhang R, Li D, Gao MQ. LRRC75A antisense lncRNA1 knockout attenuates inflammatory responses of bovine mammary epithelial cells. Int J Biol Sci. 2020;16(2):251–63.
13. Wang H, Wang X, Li X, Wang Q, Qing S, Zhang Y, et al. A novel long non-coding RNA regulates the immune response in MAC-T cells and contributes to bovine mastitis. FEBS J. 2019;286(9):1780–95.
14. Théry C, Amigorena S, Raposo G, Clayton A. Isolation and characterization of exosomes from cell culture supernatants and biological fluids. Current protocols in cell biology. 2006;Chap. 3:Unit 3.22..
15. Özdemir S, Altun S. Genome-wide analysis of mRNAs and lncRNAs in Mycoplasma bovis infected and non-infected bovine mammary gland tissues. Mol Cell Probes. 2020;50:101512.
16. Anders S, Huber W. Differential expression analysis for sequence count data. Genome biology. 2010;11(10):R106.
17. Love MI, Huber W, Anders S. Moderated estimation of fold change and dispersion for RNA-seq data with DESeq2. Genome biology. 2014;15(12):550.
18. Gao D, Kim J, Kim H, Phang TL, Selby H, Tan AC, et al. A survey of statistical software for analysing RNA-seq data. Human genomics. 2010;5(1):56–60.
19. Prosperi M, Salemi M, Azarian T, Milicchio F, Johnson JA, Oliva M. Unexpected Predictors of Antibiotic Resistance in Housekeeping Genes of Staphylococcus Aureus. ACM-BCB. 2019;2019:259–68.
20. Ashburner M, Ball CA, Blake JA, Botstein D, Butler H, Cherry JM, et al. Gene ontology: tool for the unification of biology. The Gene Ontology Consortium. Nat Genet. 2000;25(1):25–9.
21. Geng N, Wang X, Yu X, Wang R, Zhu Y, Zhang M, et al. Staphylococcus aureus Avoids Autophagy Clearance of Bovine Mammary Epithelial Cells by Impairing Lysosomal Function. Frontiers in immunology. 2020;11:746.
22. Chen C, Liu C, Niu Z, Li M, Zhang Y, Gao R, et al. RNA-seq analysis of the key long noncoding RNAs and mRNAs related to cognitive impairment after cardiac arrest and cardiopulmonary resuscitation. Aging. 2020;12(14):14490–505.
23. Jiang S, Chen J. WRN inhibits oxidative stress-induced apoptosis of human lensepithelial cells through ATM/p53 signaling pathway and its expression is downregulated by DNA methylation. Mol Med. 2020;26(1):68.
24. Berger ND, Stanley FKT, Moore S, Goodarzi AA. ATM-dependent pathways of chromatin remodelling and oxidative DNA damage responses. Philos Trans R Soc Lond B Biol Sci. 2017;372(1731):20160283.

Figures

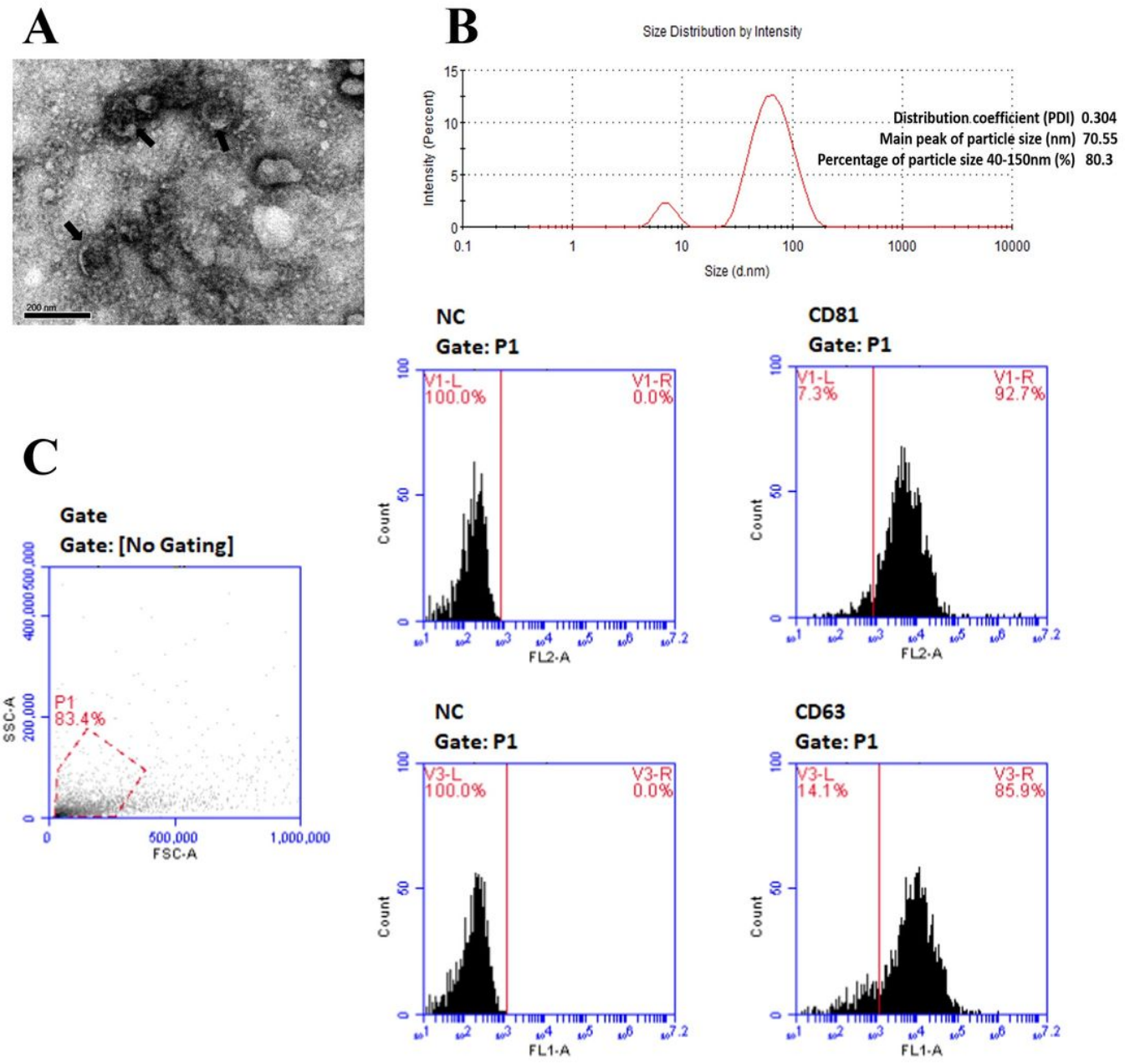

Figure 1

Identification of exosomes. (A) The morphology of exosomes under transmission electron microscope. (B) Exosomal particle size analysis was measured by NTA instrument. (C) Exosomal characteristic markers CD81 and CD63 were detected by flow cytometry. NC was negative control, P1 was gate.

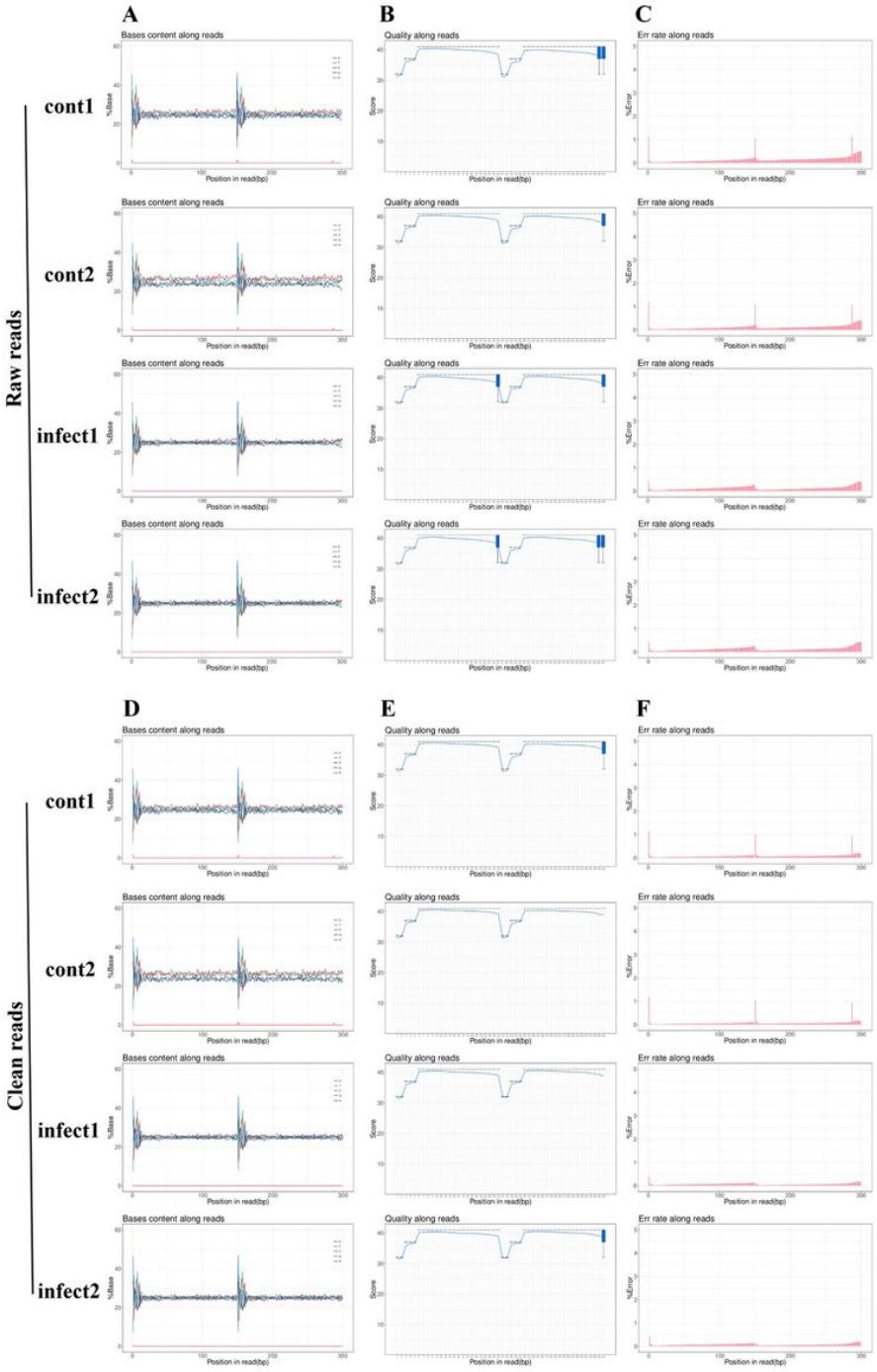

Figure 2

Sequencing data quality control. (A-C) Raw data quality control. (A) Composition of bases in each cycle. (B) The base quality distribution box plot. (C) Base error rate in raw reads. (D-F) Clean data quality control. (D) Composition of bases in each cycle. (E) The base quality distribution box plot. (F) Base error rate in raw reads.

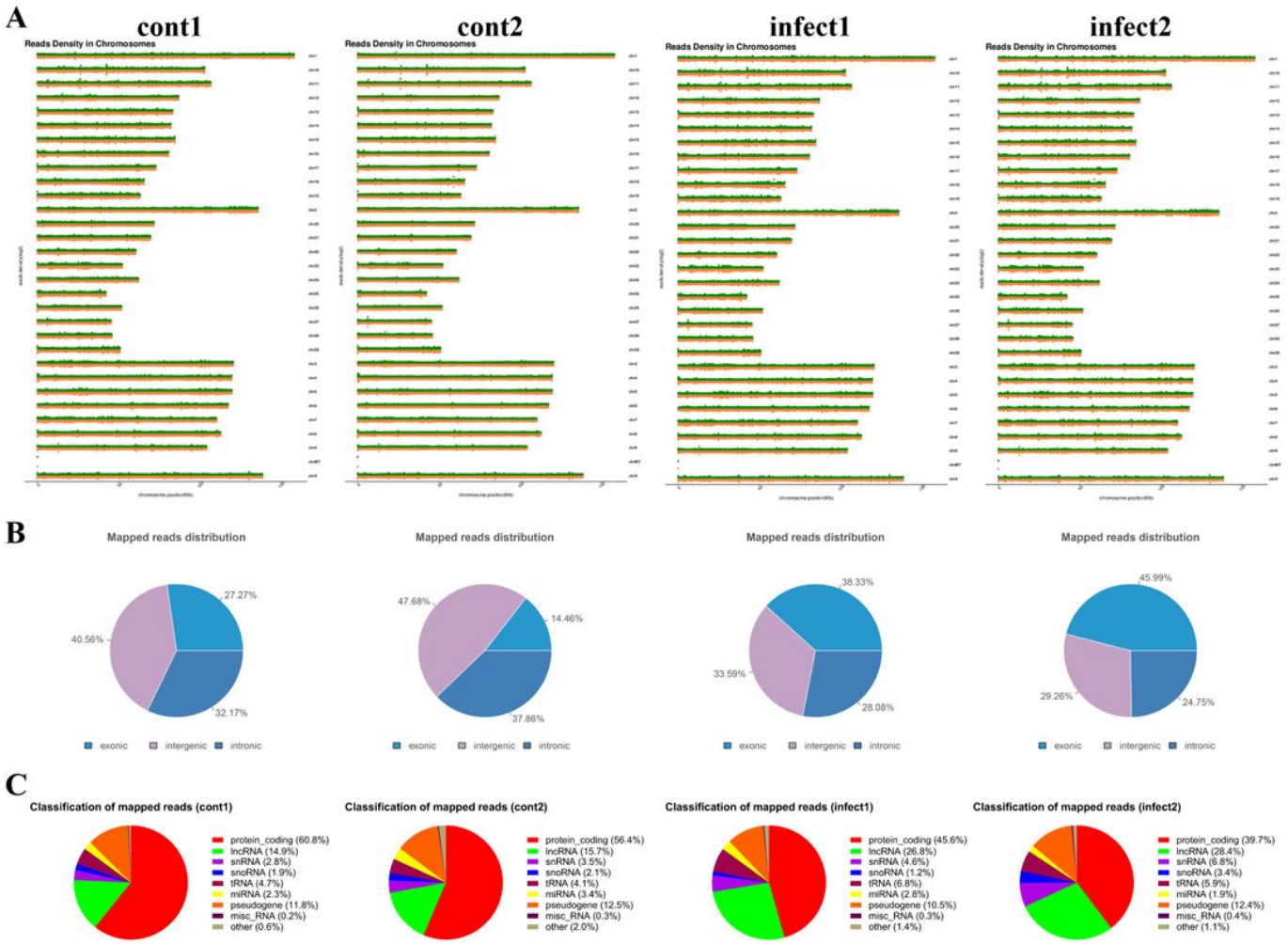

Figure 3

Mapped reads in the reference genome. (A) Distribution of reads in chromosome. (B) Location of reads in exonic, intronic, and intergenic. (C) RNA types of reads.

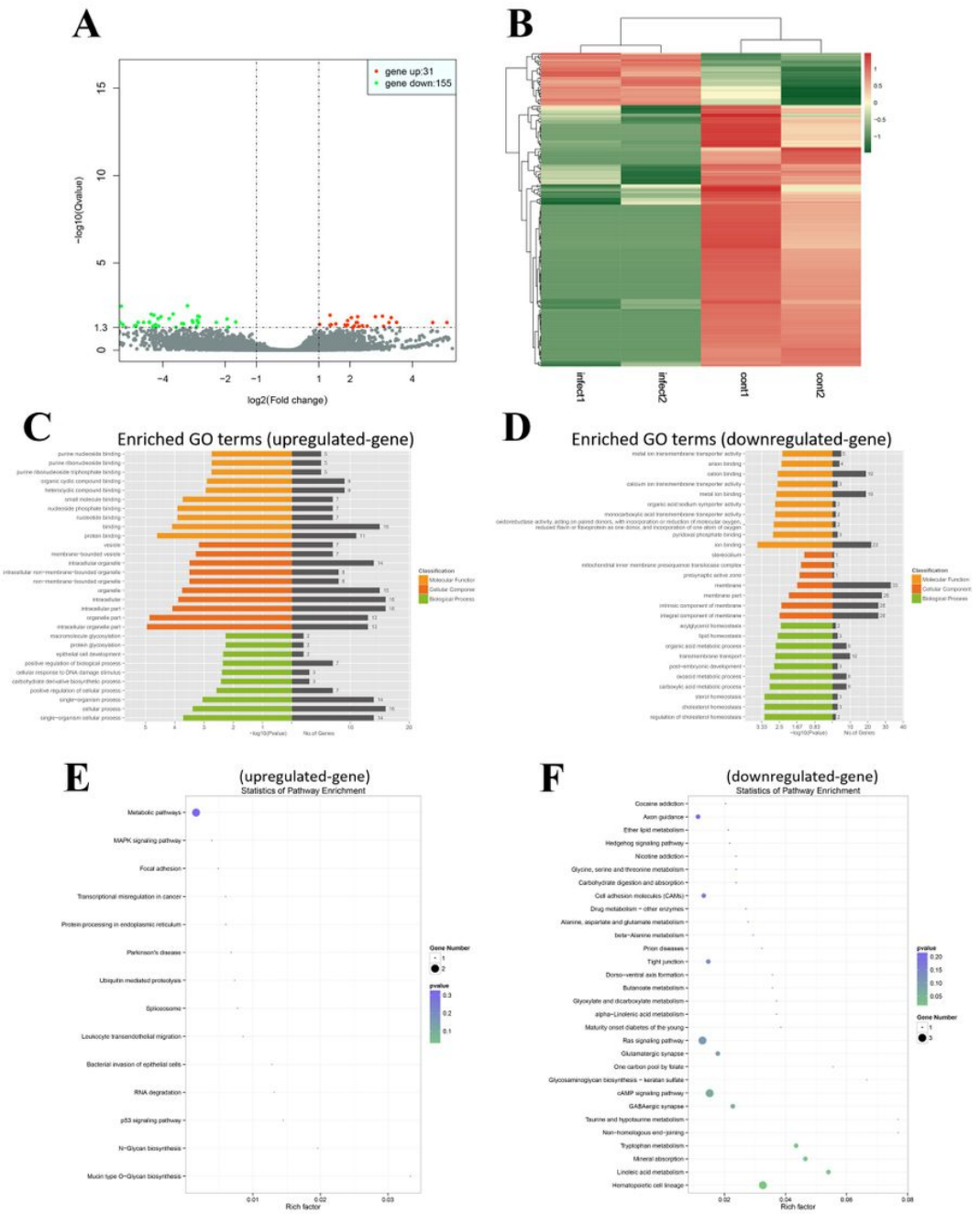

Figure 4

Differentially expressed genes analysis. (A) Volcano plot of differential expression gene. Red color represents genes with higher expression, green color represents genes with lower expression. (B) Clustering of differential expressed genes. Hierarchical clustering based on FPKMs, where log10(FPKM+1) is used for clustering. Red color represents genes with higher expression, while blue color represents genes with lower expression. (C) GO enrichment analysis on up-regulated genes. (D) GO enrichment analysis on down-regulated genes. (E) The KEGG pathway enrichment analysis on up-regulated genes. (F) The KEGG pathway enrichment analysis on down-regulated genes.

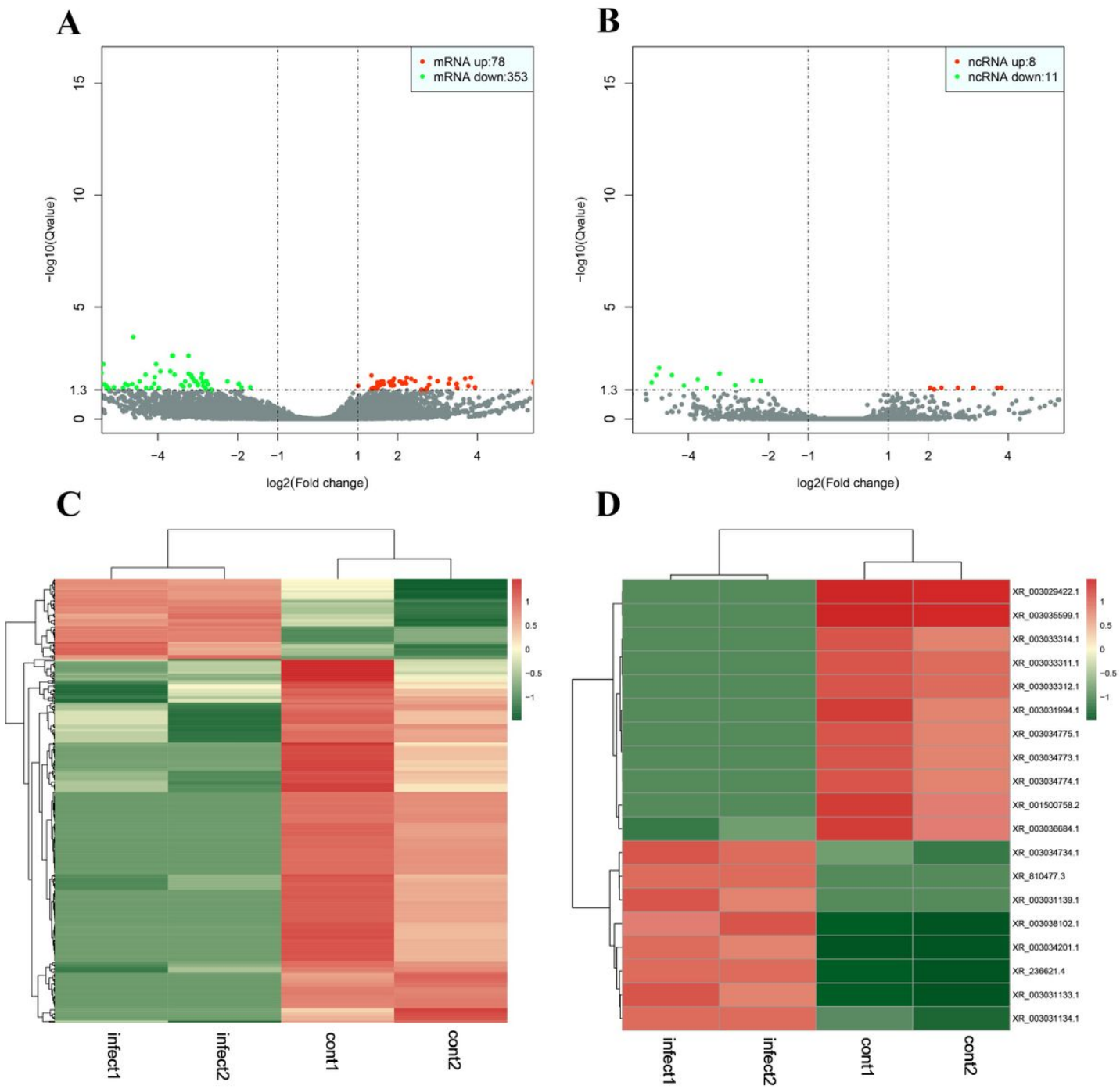

Figure 5

Differentially expressed mRNAs and lncRNAs. (A) Volcano plot of differential expression mRNA transcripts. (B) Volcano plot of differential expression lncRNA transcripts. Red color represents genes with higher expression, green color represents genes with lower expression. (C) Clustering of differential expressed mRNA. (D) Clustering of differential expressed lncRNA. Hierarchical clustering based on FPKMs, where log10(FPKM+1) is used for clustering. Red color represents genes with higher expression, while blue color represents genes with lower expression.

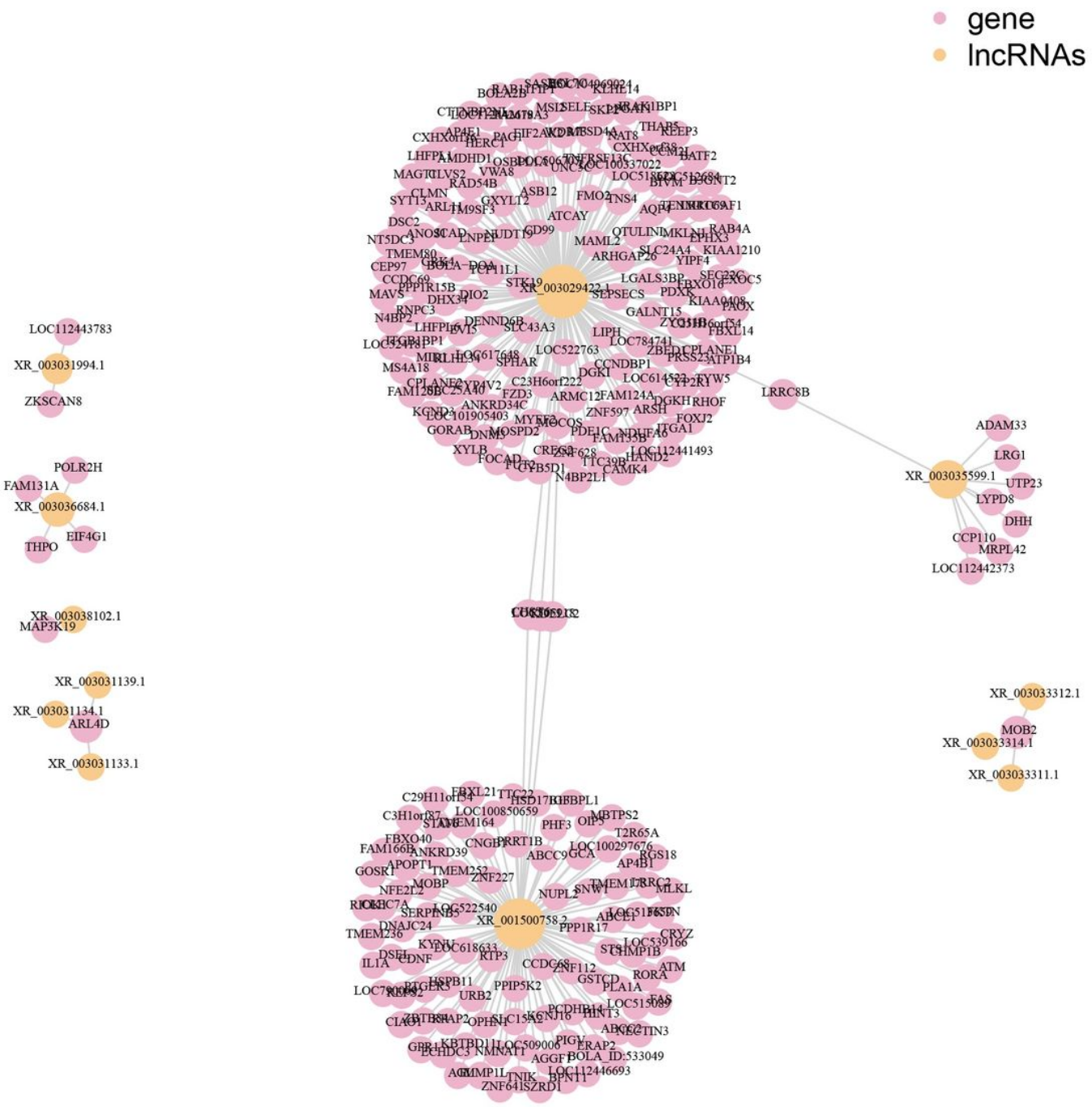

Figure 6

Network diagram of the interaction between lncRNA and target genes.

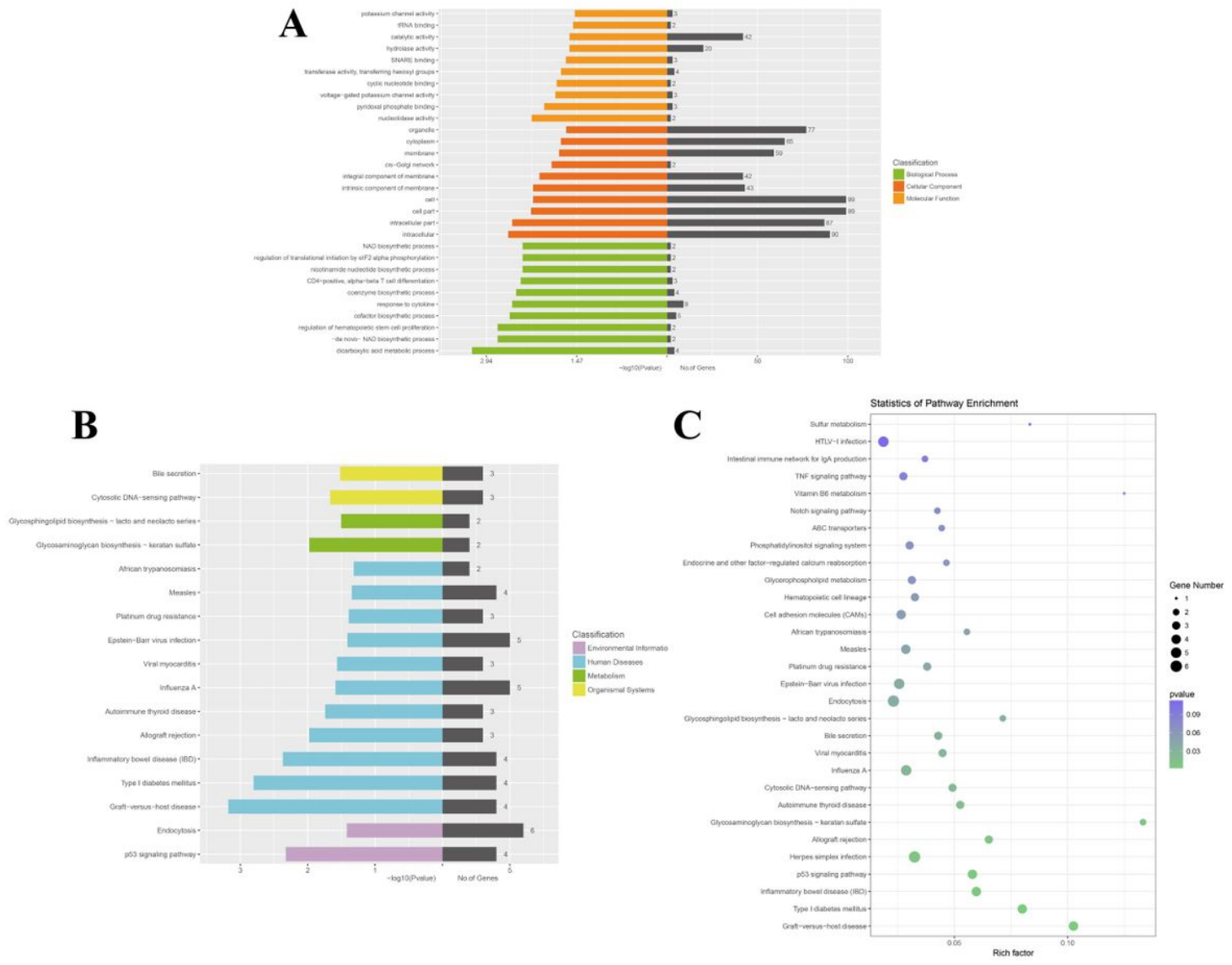

Figure 7

GO enrichment and KEGG enrichment analysis of lncRNA target genes and mRNAs. (A) GO enrichment analysis on lncRNA target genes. (B) lncRNA target genes KEGG enrichment on environmental information processing, human diseases, metabolism, and biological systems. (C) The KEGG pathway enrichment analysis on lncRNA target genes.

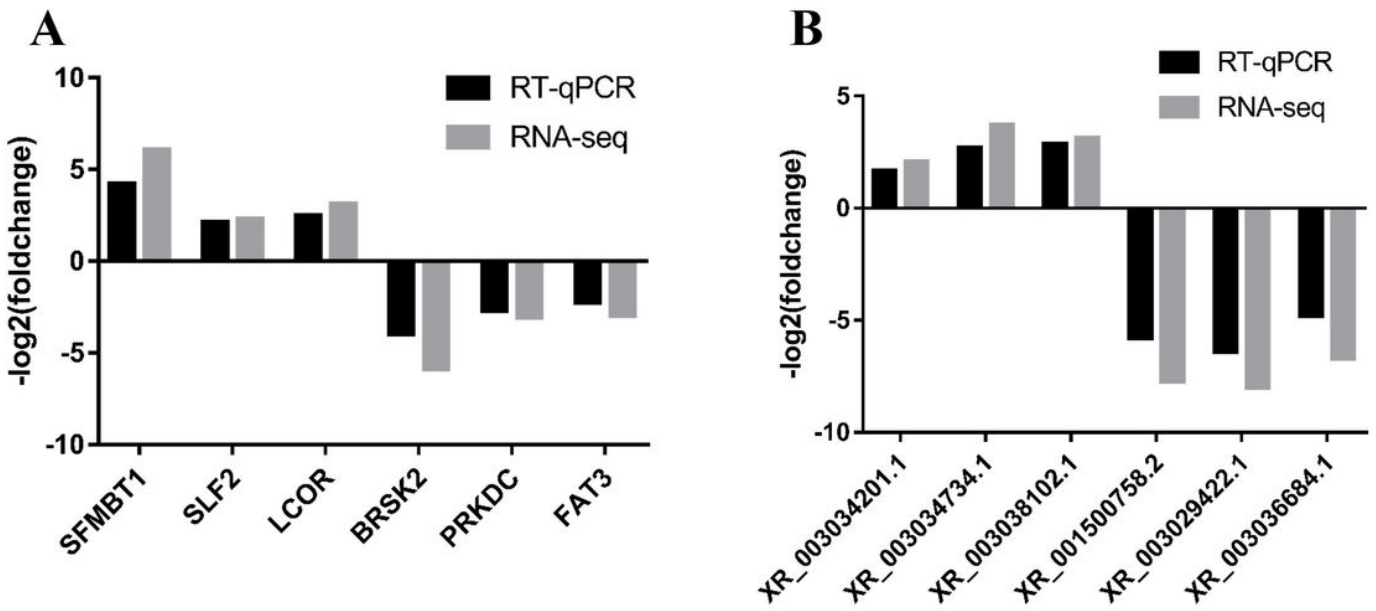

Figure 8

Comparison of relative expression of six selected differentially expressed mRNAs and lncRNAs between RT-qPCR and lncRNA-seq. (A) The relative expression level of selected mRNAs and lncRNAs were measured by RT-qPCR. (B) The relative expression level of selected lncRNAs were measured by RT-qPCR.

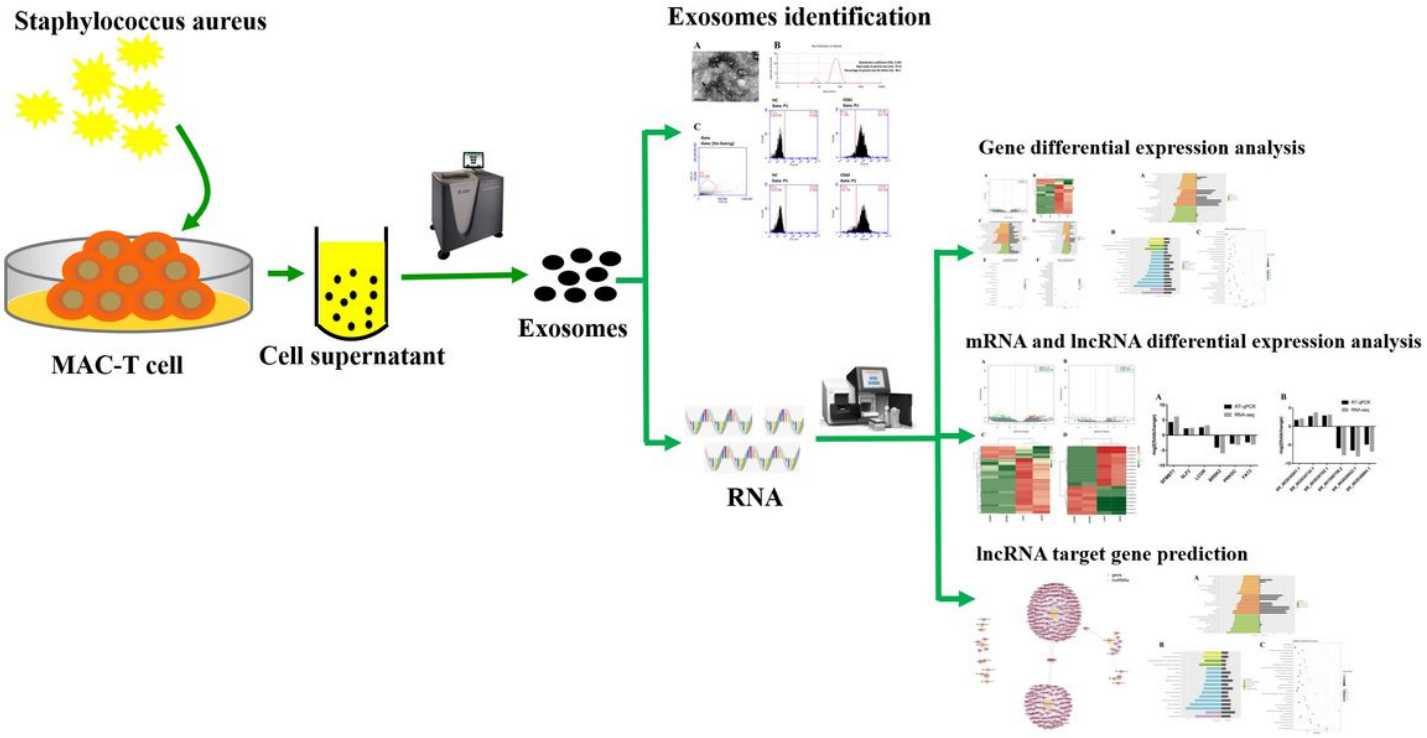

Figure 9

Schematic diagram of experimental process.

Supplementary Files

This is a list of supplementary files associated with this preprint. Click to download.

- Additionalfile5.xls
- Additionalfile4.xls
- Additionalfile3.xls
- Additionalfile2.xls
- Additionalfile1.xls